

# Interaction-Induced Weakening of Localization in Few-Particle Disordered Heisenberg Chains

Daniel Schmidtke,<sup>1,\*</sup> Robin Steinigeweg,<sup>1,†</sup> Jacek Herbrych,<sup>2,‡</sup> and Jochen Gemmer<sup>1,§</sup>

<sup>1</sup>*Department of Physics, University of Osnabrück, D-49069 Osnabrück, Germany*

<sup>2</sup>*Cretan Center for Quantum Complexity and Nanotechnology,*

*Department of Physics, University of Crete, GR-71003 Heraklion, Greece*

We investigate real-space localization in the few-particle regime of the XXZ spin-1/2 chain with a random magnetic field. Our investigation focuses on the time evolution of the spatial variance of non-equilibrium densities, as resulting for a specific class of initial states, namely, pure product states of domain-wall type. Varying the strength of both particle-particle interactions and disorder, we numerically calculate the long-time evolution of the spatial variance. For the two-particle case, our results indicate that interactions lead to an increased but still finite localization length for all parameters considered. We find that this interaction-induced increase is the stronger the more particles are taken into account in the initial condition. We further find that our non-equilibrium dynamics are clearly inconsistent with normal diffusion and instead point to subdiffusive dynamics.

PACS numbers: 05.60.Gg, 71.27.+a, 75.10.Jm

*Introduction.* Non-interacting particles in a disordered potential are Anderson-localized in one dimension (1D), for any disorder strength and temperature [1–4]. Recently, it has become clear that Anderson localization is also stable against weak particle-particle interactions [5, 6]. Moreover, numerous works suggest the existence of a many-body localized (MBL) phase beyond the weak-interaction limit and even at infinite temperature [7–9]. This MBL phase is a new state of matter with several fascinating properties, ranging from the breakdown of eigenstate thermalization [10–14] to the logarithmic growth of entanglement as a function of time, after an initial quantum quench [15–17]. In particular the optical conductivity features a zero dc value [18–20] and a low-frequency behavior as described by Mott’s law [18]. On the experimental side, an MBL phase was recently observed for interacting fermions in a quasi-random optical lattice [21, 22] as also delocalization by coupling identical 1D MBL systems [23]. Investigations of amorphous iridium-oxide indicate that MBL might play an important role for its insulating states at finite temperature [24].

The existence of a MBL phase at finite disorder and interaction strength implies that the decrease of disorder induces a transition from a localized phase (non-ergodic, non-thermal) to a delocalized phase (ergodic, thermal) [25]. This disorder-induced transition has been under active scrutiny and different probes have been suggested [26] such as subdiffusive power laws in the vicinity of the critical disorder [18], which may or may not exist [19, 27–32]. So far, a full understanding of the MBL transition is still lacking. This lack of knowledge is also related to restrictions of state-of-the-art numerical methods. On the one hand, full exact diagonalization is restricted to small systems with only a few lattice sites, where finite-size effects are strong in disorder-free cases [33–35]. On the other hand, much more sophisticated methods such as time-dependent density-matrix renormalization group

are restricted to times scales with sufficiently low entanglement [36].

While the overwhelming majority of works has focused on the disorder-induced transition at half filling, much less is known on the transition induced by filling at fixed disorder strength. Since a single particle is localized for any finite disorder, a transition from a localized phase to a delocalized phase has to occur, if the half-filling sector is delocalized. However, *when* and *how* such a transition happens exactly constitutes a non-trivial and challenging question. In particular, is it possible to break localization once the single-particle sector is left (while still far below the half-filling sector)? If so, what kind of dynamics is to be expected? If not, what is the actual effect on the localization length?

In this Letter, we study these questions for the XXZ spin-1/2 Heisenberg chain. To this end, we consider a non-equilibrium scenario, as shown in Fig. 1. First, we prepare a pure initial state of domain-wall type [37, 38], where all particles ( $\uparrow$ -spins) are concentrated at adjacent sites and holes ( $\downarrow$ -spins) are located on the other sites. Then, we calculate the evolution of the particle distribution in real time and real space, using a Runge-Kutta integration of the time-dependent Schrödinger equation, see [33, 34, 39, 40]. While the time dependence of the distribution width allows us to study the type of dynamics in general, a convergence of this width to a constant value in the long-time limit (which may or may not exist) also allows us to extract a finite localization length. To eliminate that this length is a trivial boundary effect, see Fig. 1 (inset), we choose large system sizes. The latter are feasible for different particle numbers due to our integration scheme.

We show that (i) our non-equilibrium dynamics in the few-particle regime are clearly inconsistent with normal diffusion and instead point to subdiffusive dynamics. For the two-particle case, our numerical results indicate that

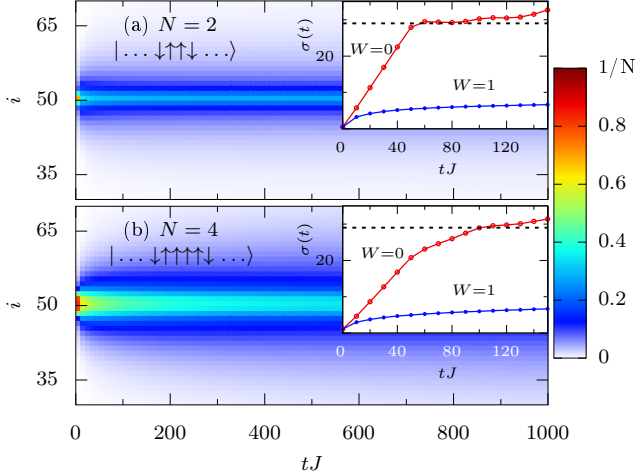


FIG. 1. (Color online) Density profile  $\langle n_i(t) \rangle$  vs. site  $i$  and time  $t$  for (a)  $N = 2$  ( $r = 10000$ ) and (b)  $N = 4$  ( $r = 1200$ ) particles, as calculated for  $L = 100$  lattice sites, interaction  $\Delta = 1$ , and disorder  $W/J = 1$ . Insets: Time dependence of the corresponding width  $\sigma(t)$  for  $W/J = 1$  as well as  $W/J = 0$ . Horizontal lines are guides to the eye.

interactions (ii) lead to an increased but (iii) still finite localization length for all parameters considered. We find that (iv) this interaction-induced increase is the stronger the more particles are taken into account in the initial condition, where the localization length may even diverge. Finally, we also provide evidence that (v) the cases of non-interacting and interacting particles can be distinguished in terms of local density correlations. Our corresponding results further suggest that (vi) particles cannot move independently and stay close to each other during the time evolution. Hence, our results shed light on the dynamics in disordered quantum systems, beyond known results at half-filling.

*Model and Non-Equilibrium Densities.* We study the XXZ spin-1/2 chain with a random magnetic field oriented in  $z$  direction. The Hamiltonian reads (with periodic boundary conditions)

$$H = \sum_{i=1}^L [J(S_i^x S_{i+1}^x + S_i^y S_{i+1}^y + \Delta S_i^z S_{i+1}^z) + h_i S_i^z], \quad (1)$$

where  $S_i^{x,y,z}$  are spin-1/2 operators at site  $i$ ,  $L$  is the number of sites,  $J > 0$  is the antiferromagnetic exchange coupling constant, and  $\Delta$  is the exchange anisotropy. The local magnetic fields  $h_i$  are random numbers drawn from a uniform distribution in the interval  $h_i \in [-W, W]$ . We note that, via the Jordan-Wigner transformation [41], this model can be mapped onto a one-dimensional model of spinless fermions with particle-particle interactions of strength  $\Delta$  and a random on-site potential of strength  $h_i$ . We are interested in the time evolution of the density

distribution

$$\langle n_i(t) \rangle = \frac{1}{N} \text{tr}[n_i \rho(t)], \quad \sum_{i=1}^L \langle n_i(t) \rangle = 1, \quad (2)$$

where  $N$  is the number of particles,  $n_i = S_i^z + 1/2$  is the occupation-number operator at site  $i$ , and  $\rho(t)$  is the density matrix at time  $t$ . In this way, we can investigate the time-dependent broadening of an initial state  $\rho(0)$  in real space, see Fig. 1. In the few-particle regime  $N \ll L/2$  studied in this paper, due to short-range interactions, only initial states with a sharp concentration of particles at adjacent sites are appropriate. For such “narrow” initial states we can expect non-trivial dynamics, while “broad” initial states essentially correspond to the one-particle problem. Thus, our initial states  $\rho(0) = |\psi(0)\rangle\langle\psi(0)|$  read (in the Ising basis)

$$|\psi(0)\rangle = \prod_{i=p}^{p+N-1} S_i^+ |\downarrow \dots \downarrow \rangle = |\downarrow \dots \downarrow \underbrace{\uparrow \dots \uparrow}_{N} \downarrow \dots \downarrow \rangle, \quad (3)$$

where  $S_i^+$  is the creation operator at site  $i$  and  $p$  is chosen to concentrate particles ( $\uparrow$ -spins) around  $i = L/2$ . These pure states of domain-wall type [37] describe an alignment of  $N$  particles directly next to each other. Note that, due to periodic boundary conditions, the specific choice of  $p$  is irrelevant.

A central quantity of our paper is the spatial variance

$$\sigma^2(t) = \sum_{i=1}^L i^2 \langle n_i(t) \rangle - \left( \sum_{i=1}^L i \langle n_i(t) \rangle \right)^2. \quad (4)$$

On the one hand, the time dependence of  $\sigma(t)$  yields information on the type of dynamics such as power laws  $t^\alpha$  for sub- ( $\alpha < 1/2$ ), normal ( $\alpha = 1/2$ ), or super-diffusion ( $\alpha > 1/2$ ). On the other hand, we can use the long-time value  $l = \lim_{t \rightarrow \infty} \sigma(t)$  as a natural definition for the localization length. Since  $l$ , as well as all other quantities introduced, depend on the specific disorder realization considered, we average over a sufficiently large number of disorder realizations  $r$ , typically  $r > 1000$ , to determine the mean of  $l$  within negligible statistical errors, see [42] for details. To also ensure negligibly small finite-size effects, we set  $L = 100$  throughout this paper. We checked that such  $L$  is sufficiently large for all quantities and time scales investigated here. Thus, for the two-particle case, i.e.,  $N = 2$ , (with Hilbert-space dimension  $\text{dim}\mathcal{H} = 4950$ ), we use full exact diagonalization (ED). For larger  $N$ , e.g.,  $N = 3$  ( $\text{dim}\mathcal{H} = 161700$ ), we rely on a forward iteration of the pure state  $|\psi(t)\rangle$  using fourth-order Runge-Kutta with a time step  $tJ = 0.01 \ll 1$ , feasible for  $L = 100$  due to sparse-matrix representations of operators, see [33, 34, 40] for details. As demonstrated below, the results obtained from this iterative method coincide for  $N = 2$  with the ED results.

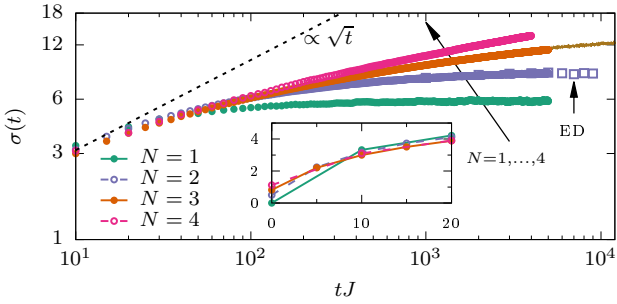


FIG. 2. (Color online) Log-log plot of the time evolution of the width  $\sigma(t)$  for different particle numbers  $N = 1, \dots, 4$  for the same parameters as in Fig. 1. For the  $N = 2$  case, corresponding ED results are also shown. For the  $N = 3$  case, long-time data for fewer  $r \approx 100$  is further depicted. A diffusive power law  $\propto \sqrt{t}$  is indicated for comparison. Inset: Lin-lin plot for short times.

*Scaling of the Variance.* Now, we present our results, starting with the time evolution of the width  $\sigma(t)$  and focusing on the isotropic point  $\Delta = 1$  and intermediate disorder  $W/J = 1$ . Fig. 2 summarizes  $\sigma(t)$  for different particle numbers  $N = 1, 2, 3$ , and 4 in a log-log plot, with statistical errors smaller than the symbol size used.

Several comments are in order. First, in the long-time limit,  $\sigma(t)$  increases monotonously as  $N$  increases from 1 to 4. Second, for  $N = 1$  and 2,  $\sigma(t)$  is approximately time-independent for  $tJ > 1000$  and takes on a constant value  $\sigma < 10$ , much smaller than the size of the lattice  $L = 100$ . On the one hand, the saturation for  $N = 1$  is expected since in this case the actual value of  $\Delta$  is irrelevant and single-particle Anderson localization persists [1, 43]. On the other hand, the saturation for  $N = 2$  is a nontrivial result. It unveils that, for our non-equilibrium domain-wall state, the proximity of another particle is not sufficient to break localization and only leads to an increase of the still finite localization length. Third, for  $N > 2$  such conclusions are less obvious. The remarkably long time scale relevant for our dynamics systematically increases with  $N$  and we do not observe a saturation of  $\sigma(t)$  at the time scales depicted in Fig. 2. Note that we have also calculated  $\sigma(t)$ , for  $N = 3$  and  $r \approx 100$ , up to very long  $tJ = 12000$ , where it still increases significantly, see Fig. 2. This ongoing increase could be a signature of a diverging localization length and would be consistent with the delocalized phase at  $N = L/2$  for this choice of  $\Delta$  and  $W$ . Finally, the time dependence of  $\sigma(t)$  is for all cases inconsistent with normal diffusion, evident when comparing  $\sigma(t)$  with the simple power law  $t^{1/2}$  indicated in Fig. 2.

In clear contrast, for short times,  $\sigma(t)$  in the inset of Fig. 2 is larger for smaller  $N$ , inverse to the long-time behavior discussed so far. This short-time behavior simply reflects that fewer particles expand in a more empty lattice. Here, disorder is not relevant yet.

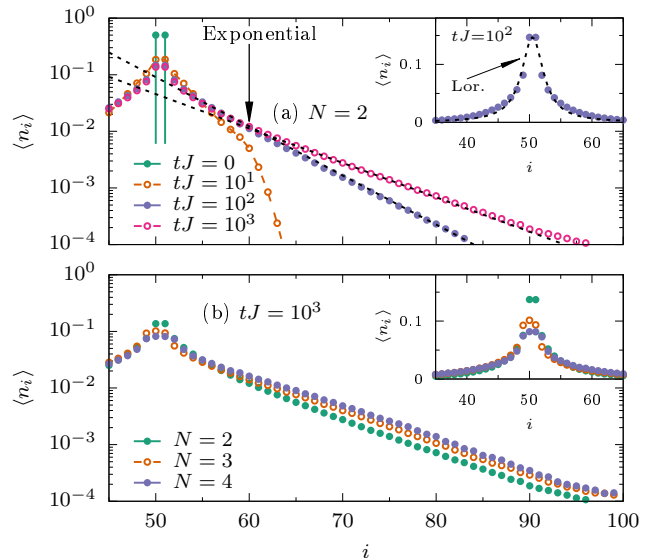


FIG. 3. (Color online) Site dependence of the density profile  $\langle n_i(t) \rangle$  at (a) times  $tJ = 0, 10, 100$ , and  $1000$  for  $N = 2$  particles and (b) at fixed time  $tJ = 1000$  for  $N = 2, 3$  and 4 particles, both in a semi-log plot. Same parameters as in Fig. 1. In (a) exponential fits to the tails are indicated. Insets: Lin-lin plots with a Lorentzian fit indicated in (a).

To gain insight into the origin of the slow dynamics of  $\sigma(t)$ , we depict in Fig. 3 time snapshots of the site dependence of the underlying density profile  $\langle n_i(t) \rangle$  for  $N = 2$  in a semi-log plot. Note that, for simplicity, we focus only on the right part of the symmetric function. Clearly, the profiles still change systematically for large times even though these changes are rather small and appear in the tails. While the profiles are well approximated by Lorentzians around their center, see inset of Fig. 3 (a), these tails show a different behavior. Remarkably, they are well described by exponentials over orders of magnitude, as expected for Anderson-localized states [1, 43],

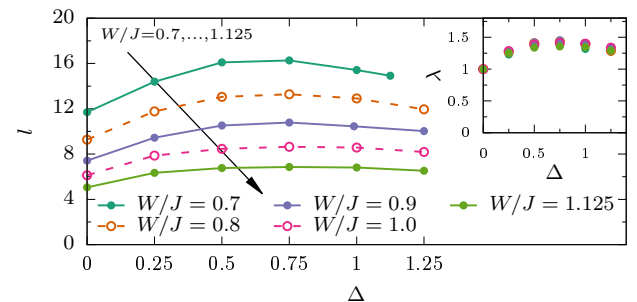


FIG. 4. (Color online) Dependence of the  $N = 2$  localization length  $l$  on the interaction strength  $\Delta$  for various disorders  $W$ , as obtained from  $\sigma(t)$  at times  $tJ = 5000$ . Inset: The same data as in main panel but for the relative localization length  $\lambda = l(\Delta)/l(\Delta = 0)$ .

but here for  $N > 1$ . We have found similar behavior for  $N = 3$  and 4. In fact, as shown in Fig. 3 (b), the spatial decay appears to be very similar for different  $N$  at fixed  $t$ . Most notably, however, the form of the distributions shows that the dynamics of our non-equilibrium state cannot be understood in terms of regular diffusion, which has been found only in few disorder-free cases [44, 45].

*Localization Length.* Next, we turn to the localization length  $l$ . In Fig. 4 we summarize our results for the  $\Delta$  and  $W$  dependence of  $l$  for the nontrivial  $N = 2$ . For this case, we observe a clear saturation of  $\sigma(t)$  at times  $tJ = 5000$  for all  $\Delta$  and  $W$  considered, cf. Fig. 2. Thus,  $l \approx \sigma(tJ = 5000)$ .

According to Fig. 4, the localization length  $l$  is finite for all parameters depicted. Clearly, at fixed interaction  $\Delta$ ,  $l$  increases as disorder  $W$  is decreased. At fixed  $W$ ,  $l$  increases as  $\Delta$  is increased from zero; however, there is a maximum of  $l$  located at  $\Delta \approx 0.75$ . The decrease of  $l$  for  $\Delta > 0.75$  occurs since our initial state is an eigenstate of the Ising limit  $\Delta \rightarrow \infty$ . In fact, we find that the system stays close to its initial state for  $\Delta > 2$ , even though not shown explicitly here. This might be seen as running into localized states comparable to Mott states [46].

While it is clear from Fig. 2 that interactions increase the localization length, it is instructive to quantify this increase by the ratio  $\lambda = l(\Delta)/l(\Delta = 0)$ , i.e., relative to the noninteracting case. As depicted in Fig. 4 (inset),  $\lambda$  appears to be almost independently of  $W$  and is largest in the region  $\Delta \approx 0.75$  where  $\lambda \approx 1.4$ . This value of  $\lambda$  is rather small indeed. But Fig. 4 clearly suggests that localization cannot be broken by our two-particle state.

*Local Density Correlations.* Finally, we intend to shed light on the nature of the transport process and on the differences between noninteracting and interacting cases,  $\Delta = 0$  and  $\Delta \neq 0$ , respectively. To this end, we consider the local density correlator

$$C_{i,\delta}(t) = \frac{\langle n_i(t) n_{i+\delta}(t) \rangle}{\langle n_i(t) \rangle \langle n_{i+\delta}(t) \rangle} \quad (5)$$

of site  $i$  and another site in distance  $\delta$ , both at a given time  $t$ . This correlation function can be interpreted as the conditional probability to find one site occupied while knowing that the other site is occupied, in relation to the individual occupation probabilities. Hence, uncorrelated sites have  $C_{i,\delta}(t) \approx 1/2$  for large  $L$  and  $N = 2$  due to the indistinguishability of particles.

In Fig. 5 we show our  $N = 2$  results for  $C_{i,\delta}(t)$  in a color map vs. site  $i$  and distance  $\delta$  for interactions  $\Delta = 0$  and 1, focusing on long times  $tJ = 3500$  and intermediate disorder  $W/J = 1$ . For the  $\Delta = 0$  case in Fig. 4 (a), there generally is no strong enhancement of correlations. The horizontal line visible, corresponding to site  $i \approx L/2$  and arbitrary  $\delta$ , has the slightly enhanced value  $\approx 0.6$ . Note that the diagonal line is equivalent to the horizontal one. These lines are the only pronounced structures and suggest that one particle is localized at its initial position

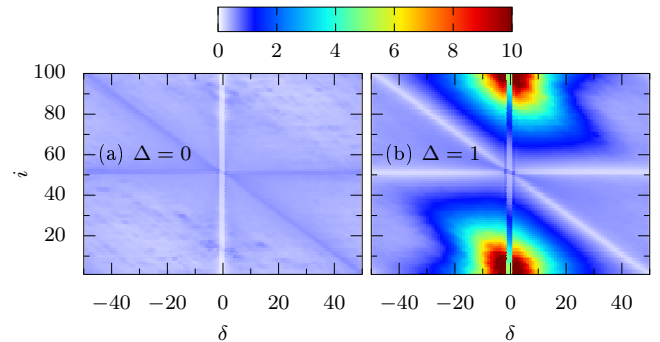


FIG. 5. (Color online) Local density correlator  $C_{i,\delta}(t)$  vs. site  $i$  and distance  $\delta$  for  $N = 2$  particles,  $W/J = 1$ , and fixed time  $tJ = 3500$ . (a) shows results for the noninteracting case  $\Delta = 0$  and (b) for the interacting case  $\Delta = 1$ .

while the other particle can move freely. For the  $\Delta = 1$  case in Fig. 5 (b), correlations are much more enhanced. A striking feature are strong correlations at  $i \ll L/2$  and  $i \gg L/2$  but with a small  $\delta$ . These correlations suggest that the two particles do not move independently and stay close to each other during the time evolution, in clear contrast to the noninteracting case  $\Delta = 0$ . This collective motion of the two particles is most likely the origin of the slow dynamics in the outer tails of the density profile discussed before.

*Conclusions.* In summary, we investigated real-space localization in the few-particle regime of the XXZ spin-1/2 chain with a random magnetic field. Our investigation focused on the time evolution of the spatial variance of non-equilibrium densities, as resulting for a specific class of initial states, namely, pure product states of domain-wall type. We showed that our non-equilibrium dynamics are clearly inconsistent with normal diffusion and instead point to subdiffusive dynamics. For the two-particle case, our numerical results indicated that interactions lead to an increased but still finite localization length for all parameters considered. We found that this interaction-induced increase is the stronger the more particles are taken into account in the initial condition. Finally, we also provided evidence that the cases of non-interacting and interacting particles can be distinguished in terms of local density correlations. Our corresponding results further suggested that interacting particles cannot move independently and stay close to each other during the time evolution. These results substantially complement known results at half filling.

*Acknowledgments.* We thank T. Prosen for fruitful discussions. J. Herbrych acknowledges support by the EU program FP7-REGPOT-2012-2013-1 under Grant No. 316165 and thanks the University of Osnabrück for kind hospitality.

---

\* [danischm@uos.de](mailto:danischm@uos.de)  
 † [rsteinig@uos.de](mailto:rsteinig@uos.de)  
 ‡ [jacek@physics.uoc.gr](mailto:jacek@physics.uoc.gr)  
 § [jgemmer@uos.de](mailto:jgemmer@uos.de)

[1] P. W. Anderson, Phys. Rev. **109**, 1492 (1958).

[2] N. F. Mott, Phil. Mag. **17**, 1259 (1968).

[3] B. Kramer and A. MacKinnon, Rep. Prog. Phys. **56**, 1469 (1993).

[4] F. Evers and A. D. Mirlin, Rev. Mod. Phys. **80**, 1355 (2008).

[5] D. M. Basko, I. L. Aleiner, and B. L. Altshuler, Ann. Phys. **321**, 1126 (2006).

[6] L. Fleishman and P. W. Anderson, Phys. Rev. B **21**, 2366 (1980).

[7] A. Pal and D. A. Huse, Phys. Rev. B **82**, 174411 (2010).

[8] V. Oganesyan and D. A. Huse, Phys. Rev. B **75**, 155111 (2007).

[9] D. J. Luitz, N. Laflorencie, and F. Alet, Phys. Rev. B **91**, 081103 (2015).

[10] M. Serbyn, Z. Papic, and D. A. Abanin, Phys. Rev. Lett. **111**, 127201 (2013).

[11] D. A. Huse, R. Nandkishore, and V. Oganesyan, Phys. Rev. B **90**, 174202 (2014).

[12] D. A. Huse, R. Nandkishore, V. Oganesyan, A. Pal, and S. L. Sondhi, Phys. Rev. B **88**, 014206 (2013).

[13] R. Nandkishore and D. A. Huse, Annu. Rev. Condens. Mat. Phys. **6**, 15 (2015).

[14] D. J. Luitz, Phys. Rev. B **93**, 134201 (2016).

[15] M. Žnidarič, T. Prosen, and P. Prelovšek, Phys. Rev. B **77**, 064426 (2008).

[16] J. H. Bardarson, F. Pollmann, and J. E. Moore, Phys. Rev. Lett. **109**, 017202 (2012).

[17] R. Vosk and E. Altman, Phys. Rev. Lett. **110**, 067204 (2013).

[18] S. Gopalakrishnan, M. Müller, V. Khemani, M. Knap, E. Demler, and D. A. Huse, Phys. Rev. B **92**, 104202 (2015).

[19] R. Steinigeweg, J. Herbrych, F. Pollmann, and W. Brenig, arXiv:1512.08519.

[20] T. C. Berkelbach and D. R. Reichman, Phys. Rev. B **81**, 224429 (2010).

[21] M. Schreiber, S. S. Hodgman, P. Bordia, H. P. Lüschen, M. H. Fischer, R. Vosk, E. Altman, U. Schneider, and I. Bloch, Science **349**, 842 (2015).

[22] S. S. Kondov, W. R. McGehee, W. Xu, and B. DeMarco, Phys. Rev. Lett. **114**, 083002 (2015).

[23] P. Bordia, H. P. Lüschen, S. S. Hodgman, M. Schreiber, I. Bloch, and U. Schneider, Phys. Rev. Lett. **116**, 140401 (2016).

[24] M. Ovadia, D. Kalok, I. Tamir, S. Mitra, B. Sacépé, and D. Shahar, Sci. Rep. **5**, 13503 (2015).

[25] J. A. Kjäll, J. H. Bardarson, and F. Pollmann, Phys. Rev. Lett. **113**, 107204 (2014).

[26] M. Filippone, P. W. Brouwer, J. Eisert, and F. von Oppen, arXiv:1606.07291.

[27] V. K. Varma, A. Lerose, F. Pietracaprina, J. Goold, and A. Scardicchio, arXiv:1511.09144.

[28] A. Karahalios, A. Metavitsiadis, X. Zotos, A. Gorczyca, and P. Prelovšek, Phys. Rev. B **79**, 024425 (2009).

[29] M. Žnidarič, A. Scardicchio, and V. K. Varma, arXiv:1604.08567.

[30] I. Khait, S. Gazit, N. Y. Yao, and A. Auerbach, Phys. Rev. B **93**, 224205 (2016).

[31] O. S. Barišć, J. Kokalj, I. Balog, and P. Prelovšek, arXiv:1603.01526.

[32] K. Agarwal, S. Gopalakrishnan, M. Knap, M. Müller, and E. Demler, Phys. Rev. Lett. **114**, 160401 (2015).

[33] R. Steinigeweg, J. Gemmer, and W. Brenig, Phys. Rev. Lett. **112**, 120601 (2014).

[34] R. Steinigeweg, J. Gemmer, and W. Brenig, Phys. Rev. B **91**, 104404 (2015).

[35] P. Prelovšek, S. E. Shawish, X. Zotos, and M. Long, Phys. Rev. B **70**, 205129 (2004).

[36] C. Karrasch, J. H. Bardarson, and J. E. Moore, Phys. Rev. Lett. **108**, 227206 (2012).

[37] J. Hauschild, F. Heidrich-Meisner, and F. Pollmann, arXiv:1605.05574.

[38] R. Steinigeweg, J. Gemmer, and M. Michel, Europhys. Lett. **75**, 406 (2006).

[39] R. Steinigeweg, J. Herbrych, X. Zotos, and W. Brenig, Phys. Rev. Lett. **116**, 017202 (2016).

[40] T. A. Elsayed and B. V. Fine, Phys. Rev. Lett. **110**, 070404 (2013).

[41] P. Jordan and E. Wigner, Z. Phys. **47**, 631 (1928).

[42] See Supplemental Material for details on statistical errors.

[43] E. Abrahams, P. W. Anderson, D. C. Licciardello, and T. V. Ramakrishnan, Phys. Rev. Lett. **42**, 673 (1979).

[44] R. Steinigeweg, EPL **97**, 67001 (2012).

[45] R. Steinigeweg, J. Herbrych, P. Prelovšek, and M. Mierzejewski, Phys. Rev. B **85**, 214409 (2012).

[46] N. F. Mott, Philos. Mag. **17**, 1259 (1968).

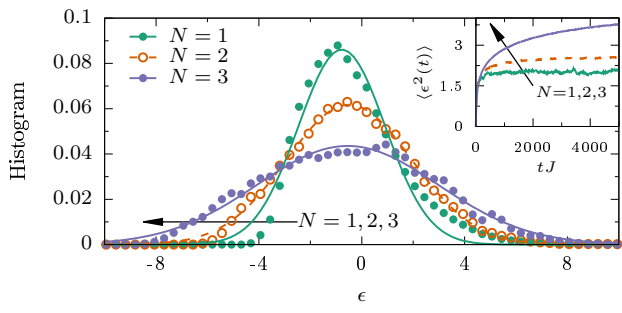


FIG. S1. (Color online) Histogram of  $\epsilon_i(t) = \sigma_i(t) - \langle \sigma(t) \rangle$  for  $N = 1, 2$ , and  $3$  at fixed  $t J = 5000$  ( $\Delta = 1$ ,  $W/J = 1$ , and  $L = 100$ ). Clearly, the overall shape is Gaussian and the width grows with  $N$ . Inset: Time evolution of  $\langle \epsilon^2(t) \rangle$  for the same parameters.

## SUPPLEMENTAL MATERIAL

### Statistical Errors

As the local magnetic fields  $h_i$  are drawn at random,  $\sigma_i(t)$  is randomly distributed around its mean  $\langle \sigma(t) \rangle$  and it is necessary to estimate statistical errors. In Fig. S1 histograms for the individual deviations  $\epsilon_i(t) =$

$\sigma_i(t) - \langle \sigma(t) \rangle$  at fixed time  $t J = 5000$ , interaction  $\Delta = 1$ , and disorder  $W/J = 1$  are shown. For  $N = 2$  and  $3$  the distributions are of Gaussian type while for  $N = 1$  the distribution is slightly asymmetric. Interestingly, the distributions become broader as the particle number is increased.

In the inset of Fig. S1 we show the time evolution of

$$\langle \epsilon^2(t) \rangle = \frac{1}{r} \sum_{i=1}^r \epsilon_i(t)^2, \quad (\text{S1})$$

for the same set of parameters. The time dependence of  $\langle \epsilon^2(t) \rangle$  is similar to the one of  $\langle \sigma(t) \rangle$  itself; however,  $\langle \epsilon^2(t) \rangle < \langle \sigma(t) \rangle$ . Furthermore, for  $N = 1$  and  $2$ , the time scale where  $\langle \epsilon^2(t) \rangle$  saturates at its maximum is also comparable. For  $N = 3$ ,  $\langle \epsilon^2(t) \rangle$  still increases in the long-time limit, just as  $\langle \sigma(t) \rangle$ .

Given the Gaussian form in Fig. S1, we can estimate the error of determining  $\langle \sigma(t) \rangle$  by  $r$  realizations from

$$\sqrt{\frac{\langle \epsilon^2(t) \rangle}{r}}. \quad (\text{S2})$$

In praxis, we choose  $r$  such large that this error is smaller than the symbol sizes used in the figures of the main text, i.e., typically  $r > 1000$ .